Dynamics of a Stratified Population of Optimum Seeking Agents on a Network - Part II : Steady State Analysis

Nirabhra Mandal and Pavankumar Tallapragada *Member, IEEE*

***Abstract*— In this second part of our work, we study the steady-state of the population and the social utility for a general class of dynamics that converge to the set of Nash equilibria and follow a certain positive correlation property. This class of dynamics includes the three dynamics introduced in the first part. We provide sufficient conditions on the network based on a maximum payoff density parameter of each node under which there exists a unique Nash equilibrium. We then utilize the positive correlation properties of the dynamics to reduce the flow graph in order to provide an upper bound on the steady-state social utility. Finally we extend the idea behind the sufficient condition for the existence of a unique Nash equilibrium to partition the graph appropriately in order to provide a lower bound on the steady-state social utility. We also illustrate interesting cases as well as our results using simulations.**

***Index Terms*— Multi-agent systems, population dynamics on networks, collective behavior, bounds on steady-state social utility.**

I. Introduction

A primary goal in the analysis of evolutionary dynamics is to characterize the set of equilibrium points and to study their stability. Many applications might also require the knowledge of the steady-state or steady-state social utility, given the initial condition of the population, for higher level control and planning problems. In this paper, we seek to obtain efficiently computable bounds on the steady-state social utility, as a function of the initial population state, under a general class of dynamics that includes *stratified smith dynamics* (SSD), *nodal best response dynamics* (NBRD) and *network restricted payoff maximization* (NRPM) [1].

A. Literature Survey

Population games and evolutionary dynamics [2] find application in problems related to distributed control and formation control [3]–[5] as well as in social or socio-technical systems such as transportation and opinion dynamics. In the context of network games, [6]–[10] model a finite population of agents as nodes and models the interactions using the graph. Other works of literature [4], [11]–[14] consider the nodes of the graph to represent choices with the state of the population being composed of the fractions of population choosing different nodes. In these works, the network plays a major role in the evolution of the population.

In the literature on distributed Nash equilibrium seeking algorithms, e.g. [15], [16], the graph models the communication network among the finitely many agents and not the underlying game. In these works, the existence and uniqueness of a Nash equilibrium is assumed and emphasis is on algorithms that drive any initial state to the Nash equilibrium.

Part one of this work [1] models the game with stratified populations with their choices as the nodes of a graph, models the three dynamics: SSD, NBRD and NRPM, studies existence and uniqueness of solutions of these dynamics and shows convergence of their solutions to the set of Nash equilibria.

B. Contribution

In this second part of our work, we first provide sufficient conditions on the graph under which the stratified population game has a unique Nash equilibrium. Then, for general graphs, we provide a computationally efficient method for computing bounds on the steady state social utility that depends on the initial population state, the network and the node parameters only. This method is particularly useful in the case of NBRD and NRPM, where simulating the full dynamics in order to determine the steady state values is computationally expensive; as these dynamics rely on an underlying optimization problem.

References [4], [12]–[14] have a setup for the underlying game closest to ours. However, they assume that Nash equilibrium is unique and in the relative interior of the n-dimensional probability simplex and results are local. Moreover, in all these works, the population is not stratified. Our preliminary work on this topic [17] considers only quadratic cumulative payoff functions as opposed to strictly concave functions and is concerned only with the convergence analysis.

C. Organization

The rest of the paper is organized as follows. In Section II, we list a few important results from the first part of this work and outline the problem we wish to address in this paper. In Section III, we give sufficient conditions on the graph under

This work was partially supported by Robert Bosch Centre for Cyber-Physical Systems, Indian Institute of Science. N. Mandal was supported by a fellowship grant from the Centre for Networked Intelligence (a Cisco CSR initiative) of the Indian Institute of Science.

N. Mandal is with the Department of Electrical Engineering, Indian Institute of Science. P. Tallapragada is with the Department of Electrical Engineering and the Robert Bosch Centre for Cyber Physical Systems, Indian Institute of Science {nirabhram, pavant}@iisc.ac.in

which the population game has a unique Nash equilibrium. In Section IV we give algorithms to provide meaningful bounds on the steady-state social utility. In Section V we provide simulation results and some interesting examples.

D. Notation and Definitions

We denote the set of real numbers, and the set of integers by $\mathbb{R}$ and $\mathbb{Z}$, respectively. We let $[p,q]_{\mathbb{Z}} := \{x \in \mathbb{Z} \,|\, p \leq x \leq q\}$. $\mathbb{R}^n$ is the cartesian product of $\mathbb{R}$ with itself n times. If $\mathbf{v}$ is a vector in $\mathbb{R}^n$, we denote $\mathbf{v}_i$ as the i^{th} component of $\mathbf{v}$ and for a vector $\mathbf{v} \in \mathbb{R}^n$, we let $\operatorname{supp}(\mathbf{v}) := \{i \in [1,n]_{\mathbb{Z}} \,|\, \mathbf{v}_i \neq 0\}$. We let $\mathbf{1}$ be the vector, of appropriate size, with all its elements equal to 1 and we let $\mathbf{e}_i$ be the vector, again of appropriate size, with its i^{th} element equal to 1 and 0 for all other elements. The empty set is denoted by $\varnothing$. If $\mathcal{Q}$ is an ordered countable set, then $\mathcal{Q}_i$ denotes the i^{th} member of $\mathcal{Q}$ and $|\mathcal{Q}|$ is used to represent the cardinality of $\mathcal{Q}$. For two sets $\mathcal{U}, \mathcal{V} \subset \mathcal{Q}$, the set subtraction operation is denoted by $\mathcal{U} \setminus \mathcal{V} = \mathcal{U} \cap \mathcal{V}^c$, where $\mathcal{V}^c$ is the set complement of $\mathcal{V}$ in $\mathcal{Q}$. $\{i,j\}$ is used to denote an unordered pair while (i,j) is used to denote an ordered pair. For a vector $\mathbf{v} \in \mathbb{R}^n$, $\mathbf{v} \geq 0$ is used to denote term wise inequalities. For a function $f(\mathbf{x}) : \mathbb{R}^n \to \mathbb{R}$, ∇f is used to denote the gradient of $f(.)$ with respect to $\mathbf{x}$, *i.e.*, the j^{th} component of ∇f is $\frac{\partial f}{\partial \mathbf{x}_j}$. We denote by $\mathcal{S}^n_\gamma$, the n-dimensional simplex $\mathcal{S}^n_\gamma := \{\mathbf{v} \in \mathbb{R}^n \mid \mathbf{v} \geq 0 \ , \ \mathbf{1}^T\mathbf{v} = \gamma\}$.

II. Preliminaries

In this section, we recollect the framework and state the essential aspects about the class of dynamics that we wish to study. We consider a *population* composed of a continuum of *agents* and a network of *choices* given by an undirected graph $\mathcal{G} := (\mathcal{V}, \mathcal{E})$ without any self loops. Here $\mathcal{V}$ is a set of nodes and $\mathcal{E} \subseteq \mathcal{V} \times \mathcal{V}$ is a set of edges. The fraction of population in node i is represented by $\mathbf{x}_i \in [0,1]$ and $\sum_{i \in \mathcal{V}} \mathbf{x}_i = 1$. Thus $\mathbf{x} \in \mathcal{S}^{|\mathcal{V}|}_1$ represents the population state.

Let $p_i(.) : [0,1] \to \mathbb{R}$ be the function that models the *cumulative payoff* of the fraction $\mathbf{x}_i$. We assume that the fraction in each node is stratified and the agents in different strata of a given node receive different payoffs. Let $[a,b] \subseteq [0,\mathbf{x}_i]$ be an arbitrary interval. Then the agents of node i that are in the *strata* $[a,b]$ get an *average payoff* of

$$\frac{p_i(b) - p_i(a)}{b - a}.$$

For a node i if $a \in [0, \mathbf{x}_i]$, then

$$u_i(a) := \frac{\mathrm{d}\, p_i}{\mathrm{d}\, y}(a)\,,$$

is the average payoff that the agents in the strata $[a]$ of node i receive. By *strata* $[a]$ we mean the collection of *infinitesimal strata* around a in $[0,\mathbf{x}_i]$. We call $u_i(.)$ as the *payoff density function* of node i. We let $u_i(0)$ be the right derivative of $p_i(.)$ at *zero* and $u_i(1)$ be the left derivative of $p_i(.)$ at *one*. We let $u(.)$ be the vector whose i^{th} element is $u_i(.)$. Through out this paper, we make the following assumption.

(A1) For all $i \in \mathcal{V}$, $p_i(.)$ is twice continuously differentiable and strictly concave. Hence, $\forall i \in \mathcal{V}$, $u_i(.)$ is a strictly decreasing function.

The function,

$$U(\mathbf{x}) := \sum_{i \in \mathcal{V}} \left[p_i(\mathbf{x}_i) - p_i(0)\right], \tag{1}$$

which we call as the *social utility function* represents the aggregate payoff of the population as a whole. Note that $U(.)$ is a strictly concave function and $\mathbf{e}_i^T \nabla U(\mathbf{x}) = u_i(\mathbf{x}_i)$, $\forall \mathbf{x} \in \mathcal{S}^{|\mathcal{V}|}_1$. We let $\mathcal{N}^i$ be the set of all neighbors of node i in the graph $\mathcal{G}$ and let $\overline{\mathcal{N}}^i = \mathcal{N}^i \cup \{i\}$. Given the undirected graph $\mathcal{G}$, we let

$$\mathcal{A} := \bigcup_{\{i,j\} \in \mathcal{E}} \{(i,j), (j,i)\}. \tag{2}$$

The dynamics that govern the evolution of the stratified population can be described by the general equation

$$\dot{\mathbf{x}} = \mathbf{J}\,\Delta(\mathbf{x}) =: \mathbf{F}(\mathbf{x})\,. \tag{3}$$

Here $\mathbf{J} \in \mathbb{R}^{|\mathcal{V}| \times |\mathcal{A}|}$ is the incidence matrix of the directed graph $\mathcal{F} := (\mathcal{V}, \mathcal{A})$ and $\Delta(\mathbf{x}) \in \mathbb{R}^{|\mathcal{A}|}$ is the vector that accumulates the *outflows* $\delta_{ij} \geq 0$ along each arc $(i,j) \in \mathcal{A}$ into a vector. Such a class of dynamics is referred to as *flow balanced dynamics*. The following lemma, which we state in [1], holds for a general case where the total population is $\rho \ \geq 0$, *i.e* $\sum_{i \in \mathcal{V}} \mathbf{x}_i = \rho$.

Lemma 2.1: (Non-emptiness of set of Nash equilibria). The unique optimizer of

$$\mathbf{P}_1(\mathcal{V}', \rho): \quad f_{\mathcal{V}'}(\rho) := \max_{\mathbf{x}} U(\mathbf{x}) \ \text{ s.t. } \ \mathbf{x} \in \mathcal{S}^{|\mathcal{V}'|}_\rho, \tag{4}$$

belongs to the set

$$\begin{aligned} \mathcal{NE}^{|\mathcal{V}'|}_\rho := \big\{\mathbf{x} \in \mathcal{S}^{|\mathcal{V}'|}_\rho \;\big|\; & u_i(\mathbf{x}_i) \geq u_j(\mathbf{x}_j), \\ & \forall\, j \in \mathcal{N}^i, \forall\, i \in \operatorname{supp}(\mathbf{x})\big\}. \end{aligned} \tag{5}$$

Hence $\mathcal{NE}^{|\mathcal{V}'|}_\rho$ is non-empty. $\bullet$

The set $\mathcal{NE}^{|\mathcal{V}'|}_\rho$ in (5) is the set of *Nash equilibria* of the population game. Next we describe the class of dynamics that we wish to study and the problem setup formally.

A. Problem Setup

In this paper, we continue our analysis of SSD, NBRD and NRPM that we started in [1]. In particular, we are interested in the steady-state behavior of these dynamics. However, the results stated in this paper hold for a general a class of flow balanced dynamics on the graph $\mathcal{G} = (\mathcal{V}, \mathcal{E})$ that satisfies the following properties.

(A2) For the dynamics (3), the simplex $\mathcal{S}^{|\mathcal{V}|}_\rho$ is positively invariant. Moreover $\forall \mathbf{x}(0) \in \mathcal{S}^{|\mathcal{V}|}_\rho$ the solution $\mathbf{x}(t)$ exists for all $t \geq 0$ and is unique.

(A3) The solution of (3) from any initial condition in $\mathcal{S}^{|\mathcal{V}|}_\rho$ asymptotically converges to the set of Nash equilibria $\mathcal{NE}^{|\mathcal{V}|}_\rho$ in (5).

(A4) If $\mathbf{x}(t)$ is the solution of (3) with an initial condition $\mathbf{x}(0) \in \mathcal{S}^{|\mathcal{V}|}_\rho$, then $U(\mathbf{x}(t))$ converges to a constant.

(A5) Let $\theta \in \mathbb{R}^{|\mathcal{V}|}$ be a vector with individual components $\theta_i \geq 0$. Then if $\mathbf{x}_i \in [0, \theta_i]$ or $\mathbf{F}_i(\mathbf{x}) + \mathbf{x}_i \in [0, \theta_i]$ then

$$\delta_{ij}(\mathbf{x}) = 0,\ \forall (i,j) \in \mathcal{A} \text{ s.t. } u_i(\theta_i) \geq u_j(0)\,. \tag{6}$$

We seek to study the steady-state and the steady-state social utility with the knowledge of the structure of the graph $\mathcal{G} = (\mathcal{V}, \mathcal{E})$ and the initial condition, $\mathbf{x}^0 := \mathbf{x}(0)$.

We call any dynamics that follows Assumptions **(A2)** and **(A3)** as *Nash convergent dynamics*.Since by Assumption **(A4)**, the social utility converges to a constant value, we let $U_{\text{ss}}(\mathbf{x}^0)$ to be the value to which the social utility converges to under the flow balanced dynamics from an initial condition $\mathbf{x}^0$. In Section III, we give a sufficient condition under which the steady-state of any dynamics that follows Assumptions **(A2)** and **(A3)** (*i.e. Nash convergent dynamics*) is the same. Then in Section IV, we provide bounds on the steady-state social utility for any dynamics that follows Assumptions **(A2)** - **(A5)**.

We end this section by stating that SSD, NBRD and NRPM satisfy **(A2)** - **(A5)**. We prove this result in Appendix II-A.

Lemma 2.2: (Properties SSD, NBRD and NRPM). Suppose Assumption **(A1)** holds. Consider the dynamics SSD, NBRD and NRPM proposed in [1] on the graph $\mathcal{G} = (\mathcal{V}, \mathcal{E})$ with an initial condition $\mathbf{x}(0) \in \mathcal{S}_\rho^{|\mathcal{V}|}$. All three dynamics satisfy **(A2)** - **(A5)**. Further, if $\mathbf{x}(t)$ is the unique solution from the initial condition, then $U(\mathbf{x}(t))$ is a non-decreasing function of t. •

III. Unique Nash Equilibrium

In this section, we give sufficient conditions on the graph $\mathcal{G}$ and the payoff density functions, under which the set of Nash equilibria is a singleton. We define for each node $i \in \mathcal{V}$, the *maximum payoff density parameter* (MPDP) as

$$\mathbf{a}_i := \max_{y \in [0,1]} u_i(y) = u_i(0), \tag{7}$$

where we use the fact that $u_i(.)$ is a strictly decreasing function in $[0, 1]$ for all $i \in \mathcal{V}$.

We formally define a path in a graph next.

Definition 3.1: (Path in a graph $\mathcal{G}' = (\mathcal{V}', \mathcal{E}')$). A path, in a graph $\mathcal{G}' = (\mathcal{V}', \mathcal{E}')$, between $i \in \mathcal{V}'$ and $j \in \mathcal{V}'$ is given by an ordered set of non-repeating elements $\mathcal{P}(i, j) \subseteq \mathcal{V}'$ such that $\mathcal{P}_1(i, j) = i$, $\mathcal{P}_n(i, j) = j$ and $\{\mathcal{P}_k(i, j), \mathcal{P}_{k+1}(i, j)\} \in \mathcal{E}$, $\forall k \in [1, n-1]_{\mathbb{Z}}$. Here $\mathcal{P}_k(i, j)$ denotes the k^{th} element in $\mathcal{P}(i, j)$ and $n = |\mathcal{P}(i, j)|$. •

Using this definition and (7), we define a *path with quasi-concave MPDP's* next.

Definition 3.2: (Path with quasi-concave MPDP's). Suppose $\mathcal{P}(i, j)$ is a path, in a graph $\mathcal{G}' = (\mathcal{V}', \mathcal{E}')$, between $i \in \mathcal{V}'$ and $j \in \mathcal{V}'$ and let $n := |\mathcal{P}(i, j)|$. Let $\pi(k) := \mathcal{P}_k(i, j)$. We say $\mathcal{P}(i, j)$ is a path with quasi-concave MPDP's if and only if $\forall\, k, l \in [1, n]_{\mathbb{Z}}$ such that $l \geq k$ and $\forall m \in [k, l]_{\mathbb{Z}}$, $\mathbf{a}_{\pi(m)} \geq \min\{\mathbf{a}_{\pi(k)}, \mathbf{a}_{\pi(l)}\}$. •

Definition 3.2 can be interpreted in the following way. For a path with quasi-concave MPDP's, if we arrange the MPDP's in order of the nodes visited in the path, then the MPDP's form a quasi-concave function. Using this interpretation and Definition 3.2, the following result can be immediately stated regarding the nature of MPDP's in such a path.

Lemma 3.3: (Monotonicity of MPDP's in a path with quasi-concave MPDP's). Let $\mathcal{P}(i, j)$ be a path with quasi-concave MPDP's between i and j, where $i, j \in \mathcal{V}$. Let $\pi(k) := \mathcal{P}_k(i, j)$ and $n = |\mathcal{P}(i, j)|$. Then $\forall\, k \in [1, n]_{\mathbb{Z}}$, either $\mathbf{a}_i = \mathbf{a}_{\pi(1)} \leq \mathbf{a}_{\pi(2)} \leq \cdots \mathbf{a}_{\pi(k)}$ or $\mathbf{a}_{\pi(k)} \geq \cdots \geq \mathbf{a}_{\pi(n-1)} \geq \mathbf{a}_{\pi(n)} = \mathbf{a}_j$. •

A proof of this is provided in Appendix II-B.1.

Using Definition 3.2, we define a *quasi-concave hill* next.

Definition 3.4: (Quasi-concave hill or QCH). We call a graph $\mathcal{G}' = (\mathcal{V}', \mathcal{E}')$ a quasi-concave hill or QCH if and only if there exists a path with quasi-concave MPDP's between every two nodes $i, j \in \mathcal{V}'$. •

Note that Definition 3.4 requires the graph $\mathcal{G}'$ to be connected. The 'hill' in QCH is given to evoke the interpretation that the agents are always seeking to climb a hill to increase their payoffs. The following lemma shows that in a QCH, if the population is in a Nash equilibrium state, then the payoff densities across the non-empty nodes is the same. We present the proof in Appendix II-B.2.

Lemma 3.5: (Same payoff density across non-empty nodes at Nash equilibrium in a QCH). Let $\mathcal{G} = (\mathcal{V}, \mathcal{E})$ be a QCH and let $\mathbf{x} \in \mathcal{NE}_\rho^{|\mathcal{V}|}$. Then $\forall\, i, j \in \text{supp}(\mathbf{x})$, $u_i(\mathbf{x}_i) = u_j(\mathbf{x}_j)$.•

Finally in this section we show that for a QCH, the Nash equilibrium is unique. We illustrate the consequence of this fact in the remark following the theorem, proof of which is presented in Appendix II-B.3

Theorem 3.6: (Uniqueness of Nash equilibrium for a QCH). Suppose $\rho \geq 0$. If $\mathcal{G} = (\mathcal{V}, \mathcal{E})$ is a QCH then $\mathcal{NE}_\rho^{|\mathcal{V}|}$ in (5) is a singleton and the unique $\mathbf{x} \in \mathcal{NE}_\rho^{|\mathcal{V}|}$ is the unique optimizer of $\mathbf{P}_1(\mathcal{V}, \rho)$ in (4). •

Remark 3.7: (Same steady-state state of Nash convergent dynamics for QCH). The immediate consequence of Theorem 3.6 is that $\forall \mathbf{x}(0) \in \mathcal{S}_\rho^{|\mathcal{V}|}$ the steady-state state of any Nash convergent dynamics is the same. •

The utility of Theorem 3.6 and Remark 3.7 extends to the case in which $\mathcal{G}$ is not a QCH. In particular, we can use them to bound the steady-state social utility of dynamics that follow Assumptions **(A2)** - **(A5)**. This is the topic of the next section.

IV. Bounds on the Steady-State Social Utility

The graph $\mathcal{G}$ being a QCH is a sufficient condition for dynamics that follow Assumptions **(A2)** - **(A5)** to share a common steady-state irrespective of the initial condition in $\mathcal{S}_\rho^{|\mathcal{V}|}$. In this section, we provide meaningful bounds on the steady-state social utility of such dynamics in the case where $\mathcal{G}$ is not a QCH. In the construction of these bounds, the results stated in Section III serve as important building blocks.

Recall that $\mathcal{G} = (\mathcal{V}, \mathcal{E})$ is the underlying undirected graph and $\mathcal{A}$ the associated arc set where for each undirected edge $\{i, j\} \in \mathcal{E}$, we have directed arcs (i, j) and (j, i) in $\mathcal{A}$. Moreover, $\mathcal{A}$ contains no other arcs. Based on the payoff functions $u_i(.)$, it is possible to reduce $\mathcal{A}$ based on the fact that some δ_{ij}'s will remain *zero* because of Assumption **(A5)** no matter what the initial condition is.

In fact, for a given initial state $\mathbf{x}(0) = \mathbf{x}^0$, if θ_i is a uniform (in time) upper bound on $\mathbf{x}_i$ or $\mathbf{F}_i(\mathbf{x}) + \mathbf{x}_i$ for each $i \in \mathcal{V}$ then for the arcs $(i, j) \in \mathcal{A}$ with the property $u_i(\theta_i) \geq u_j(0)$, the flow $\delta_{ij} = 0$ for all time $t \geq 0$ and hence the arc (i, j) can be removed without affecting the evolution of $\mathbf{x}$.

In order to reduce the graph further, the initial condition $\mathbf{x}^0$ must be taken into account. In fact, only the nodes which have a directed path in the graph $\mathcal{F} = (\mathcal{V}, \mathcal{A})$ from some node in $\text{supp}(\mathbf{x}^0)$ are the ones that may participate in the evolution of

$\mathbf{x}$. The following remark describes how Algorithm 1 utilizes Assumption **(A5)** to carry out such a reduction.

```
Algorithm 1: reduceGraph($\mathcal{F}', \mathbf{x}^0$)
   Data: $\mathcal{F}' = (\mathcal{V}', \mathcal{A}'), \mathbf{x}^0$
   Result: ICRG of $\mathcal{F}'$
1  $\mathcal{F}_{\text{red}} \leftarrow (\mathcal{V}', \mathcal{A}')$
2  $\mathcal{F}_{\text{temp}} \leftarrow (\varnothing, \varnothing)$
3  while $\mathcal{F}_{\text{red}} \neq \mathcal{F}_{\text{temp}}$ do
4      $\mathcal{F}_{\text{temp}} \leftarrow \mathcal{F}_{\text{red}}$
5      $\mathcal{F}_{\text{red}} \leftarrow$ repeatReduction $(\mathcal{F}_{\text{red}}, \mathbf{x}^0)$
6  end
7  return: $\mathcal{F}_{\text{red}}$
```

```
Algorithm 2: repeatReduction($\mathcal{F}', \mathbf{x}^0$)
   Data: $\mathcal{F}' = (\mathcal{V}', \mathcal{A}'), \mathbf{x}^0$
   Result: Reduced graph
1  for $i \in \mathcal{V}'$ do
2      $\mathcal{R}^i \leftarrow \{j \in \operatorname{supp}(\mathbf{x}^0) \mid \exists$ a directed path
                                  in $\mathcal{F}'$ from $j$ to $i\}$
3      $\theta_i \leftarrow \sum_{j \in \mathcal{R}^i} \mathbf{x}_j^0$
                        ▶ estimates the maximum population
                              fraction that can visit $i$
4  end
5  $\mathcal{A}_{\text{temp}} \leftarrow \mathcal{A}' \setminus \{(i,j) \in \mathcal{A}' \mid u_i(\theta_i) \geq u_j(0)\}$
6  $\mathcal{F}_{\text{temp}} \leftarrow (\mathcal{V}', \mathcal{A}_{\text{temp}})$
7  $\mathcal{V}_{\text{temp}} \leftarrow \operatorname{supp}(\mathbf{x}^0)$
                        ▶ $\operatorname{supp}(\mathbf{x}^0)$ is always a subset of
                              the reduced node set
8  $\mathcal{V}_{\text{temp}} \leftarrow \mathcal{V}_{\text{temp}} \cup \{i \in \mathcal{V}' \mid \exists$ a directed path in $\mathcal{F}_{\text{temp}}$
                        from some $j \in \operatorname{supp}(\mathbf{x}^0)$ to $i\}$
9  $\mathcal{A}_{\text{temp}} \leftarrow \mathcal{A}_{\text{temp}} \setminus \{(i,j) \in \mathcal{A}_{\text{temp}} \mid i \notin \mathcal{V}_{\text{temp}}$
                        or $j \notin \mathcal{V}_{\text{temp}}\}$
                              ▶ remove hanging arcs
10 return: $\mathcal{F}_{\text{temp}} = (\mathcal{V}_{\text{temp}}, \mathcal{A}_{\text{temp}})$
```

Remark 4.1: (Graph reduction using initial state). The function reduceGraph() described in Algorithm 1 takes in a directed graph $\mathcal{F}'$ and $\mathbf{x}^0$ as inputs and returns the reduced graph $\mathcal{F}_{\text{red}}$ of $\mathcal{F}'$. Algorithm 2 simultaneously estimates θ_i and removes nodes and arcs of $\mathcal{F}'$ until the graph cannot be reduced further. Steps 2-3 are used to estimate θ_i by setting it as the sum of all possible population fractions that can reach i, respecting the structure of the graph and the node parameters. Then Steps 7-9 only consider $\operatorname{supp}(\mathbf{x}^0)$ and those nodes in $\mathcal{F}'$ that have a directed path from some node in $\operatorname{supp}(\mathbf{x}^0)$. The other nodes and hanging arcs are removed. Thus, for $\mathcal{F} = (\mathcal{V}, \mathcal{A})$, reduceGraph$(\mathcal{F}, \mathbf{x}^0)$ returns the reduced graph $\hat{\mathcal{F}} = (\hat{\mathcal{V}}, \hat{\mathcal{A}})$ with the following properties:

- $\operatorname{supp}(\mathbf{x}^0)$ is contained in $\hat{\mathcal{V}}$;
- $\hat{\mathcal{A}}$ does not contain arcs (i,j) of $\mathcal{A}$ with the property $u_i(\theta_i) \geq u_j(0)$ for the estimated θ.

We call $\hat{\mathcal{F}}$ the *initial condition reduced graph* (ICRG) of $\mathcal{G}$.

Now, the fact that the Steps 2-3 of Algorithm 2 refine, with each pass, the upper bound on both $\mathbf{x}(t)$ and $\mathbf{F}(\mathbf{x}(t)) + \mathbf{x}(t)$ can be easily seen from the fact that $\mathbf{F}(\mathbf{x}(t)) + \mathbf{x}(t)$ is just a simple rearrangement of the population state $\mathbf{x}(t)$ among $\mathcal{V}$. Thus by Assumption **(A5)**, the evolution of the population under $\mathcal{G}$ is equivalent to the evolution of the population under the reduced graph $\hat{\mathcal{F}}$. •

The ICRG is useful in providing reasonable bounds on the steady-state social utility. We demonstrate this next.

A. Upper Bound on Steady-State Social Utility

In order to compute an upper bound on the steady-state social utility, we try to compute the best social utility that the population as a whole can receive starting from $\mathbf{x}^0$. This best social utility is in the space of all possible dynamics that have the property that the evolution is same under $\mathcal{G}$ and $\hat{\mathcal{F}}$. From Remark 4.1, we see that θ provided by reduceGraph$(\mathcal{F}, \mathbf{x}^0)$, Algorithm 1, is an upper bound on $\mathbf{x}(t)$ and $\mathbf{F}(\mathbf{x}(t)) + \mathbf{x}(t)$ for all $t \geq 0$. Thus, if $\hat{\mathcal{F}}$ is the ICRG of $\mathcal{G}$ and $(i,j) \notin \hat{\mathcal{A}}$ then by Assumption **(A5)** $\delta_{ij}(\mathbf{x}(t)) = 0$ for all $t \geq 0$. Moreover if $i \in \mathcal{V}$ but $i \notin \hat{\mathcal{V}}$, then $\mathbf{x}_i(t) = 0, \forall t \geq 0$. For a node $i \in \mathcal{V}$ of $\mathcal{G}$, we define the set of in-reachable nodes of i as ${}^{\text{in}}\mathcal{R}^i := \{j \in \hat{\mathcal{V}} \mid \exists$ a directed path from j to i in $\hat{\mathcal{F}}\} \cup \{i\}$ and the set of out-reachable nodes of i as ${}^{\text{out}}\mathcal{R}^i := \{j \in \hat{\mathcal{V}} \mid \exists$ a directed path from i to j in $\hat{\mathcal{F}}\} \cup \{i\}$. We use $\mathbf{r}_{ij}$ to represent the outflow from i to $j \in {}^{\text{out}}\mathcal{R}^i$ and let $\mathbf{r}$ be the vector that accumulates all the $\mathbf{r}_{ij}$ into a vector. Then the optimum value of the optimization problem $\mathbf{P}_4$ can be used as an upper bound on the steady-state utility.

$$
\mathbf{P}_4 : \quad
\begin{aligned}
U_{\max} := \max_{\mathbf{w},\mathbf{r}} & \sum_{i \in \hat{\mathcal{V}}} \left[p_i\left(\mathbf{w}_i\right) - p_i(0)\right] \\
\text{s.t. } \mathbf{w}_i = & \sum_{j \in {}^{\text{in}}\mathcal{R}^i} \mathbf{r}_{ji}, \ \forall i \in \hat{\mathcal{V}} \\
& \mathbf{r}_{ij} \geq 0, \ \forall i \in \hat{\mathcal{V}}, \ \forall j \in {}^{\text{out}}\mathcal{R}^i \\
& \sum_{j \in {}^{\text{out}}\mathcal{R}^i} \mathbf{r}_{ij} = \mathbf{x}_i^0, \ \forall i \in \hat{\mathcal{V}} .
\end{aligned}
\tag{8}
$$

Note that $\mathbf{P}_4$ is visually similar to $\mathbf{P}_3$ of NRPM in [1] but they are very different problems. In $\mathbf{P}_3$, the decision variables in $\mathbf{d}$ restricts the movement of the population fraction in each node to itself and among its neighbors in $\mathcal{G}$, *i.e.* $\mathbf{d}_{ij}$ captures the outflow form node $i \in \mathcal{V}$ to node $j \in \mathcal{N}^i$ (the neighbor set only). In $\mathbf{P}_4$, on the other hand, the decision variables in $\mathbf{r}$ allows the movement of the population fraction from each node to any node that is out-reachable from it in $\hat{\mathcal{F}}$. Thus, while $\mathbf{P}_3$ gives us the instantaneous flows in NRPM, $\mathbf{P}_4$ gives us the socially optimal longterm redistribution of the population starting from $\mathbf{x}^0$ and under the path constraints imposed by $\hat{\mathcal{F}}$.

Next, we present the main result of this section and present its proof in Appendix II-C.1.

Theorem 4.2: (Upper bound on steady-state social utility). Suppose $\mathbf{x}^0 \in \mathcal{S}_\rho^{|\mathcal{V}|}$ and the evolution of $\mathbf{x}$ is governed by (3) with Assumptions **(A2)** - **(A5)** . Then the steady-state social utility from the initial condition $\mathbf{x}^0$, $U_{\text{ss}}(\mathbf{x}^0) \leq U_{\max}$. •

In the next subsection, we provide algorithms to compute lower bounds on the steady-state social utility.

B. Lower Bound on Steady-State Social Utility

In order to provide a meaningful lower bound on the steady-state social utility, we partition the graph into certain subgraphs, each of which is a directed QCH, which we define formally in the sequel. Then, using the properties in Section III, we utilize (4) to compute the social utility of the population among each group independently for different allocations of population fractions in the group. Then, the problem is converted to one of optimal allocations to the collection of directed QCHs so that social utility is minimized.

We now formally define a directed QCH and subsequently, we also define other useful definitions. **Note:** up to the very end of this subsection, we present in the context of an arbitrary graph and in the end we apply it to ICRG $\hat{\mathcal{F}}$.

Definition 4.3: (Directed quasi-concave hill). We call a digraph to be a *directed quasi-concave hill* (DQCH) if and only if its corresponding undirected graph is a QCH. •

Definition 4.4: (Directed quasi-concave hill component or DQCH component). A subgraph $\mathcal{H} = (\mathcal{W}, \mathcal{Q})$ of a directed graph $\mathcal{F}' = (\mathcal{V}', \mathcal{A}')$ is said to be a *directed quasi-concave hill component* or *DQCH component* if and only if $\mathcal{H}$ is a DQCH. •

Each DQCH component can be classified into one of two types: *attractive* or *non-attractive*. We define these next and also describe their significance.

Definition 4.5: (Attractive DQCH component or A-DQCH component). Let $\mathcal{F}' = (\mathcal{V}', \mathcal{A}')$ be a directed graph and let ${}^{\text{out}}\mathcal{N}^i(\mathcal{F}')$ be the set of out-neighbors of a node $i \in \mathcal{V}'$ in $\mathcal{F}'$. A subgraph $\mathcal{H} = (\mathcal{W}, \mathcal{Q})$ of the graph $\mathcal{F}'$ is said to be an *attractive directed quasi-concave hill component* or *A-DQCH component* of $\mathcal{F}'$ if and only if

- $\mathcal{H}$ is a DQCH;
- ${}^{\text{out}}\mathcal{N}^i(\mathcal{F}') \subseteq \mathcal{W}$, $\forall i \in \mathcal{W}$ and $\mathcal{Q} = \{(i,j) \,|\, i \in \mathcal{W},\ j \in {}^{\text{out}}\mathcal{N}^i(\mathcal{F}')\}$. •

Definition 4.6: (Non attractive DQCH component or NA-DQCH component). Let $\mathcal{F}' = (\mathcal{V}', \mathcal{A}')$ be a directed graph and let ${}^{\text{out}}\mathcal{N}^i(\mathcal{F}')$ be the set of out-neighbors of a node $i \in \mathcal{V}'$ in $\mathcal{F}'$. A subgraph $\mathcal{H} = (\mathcal{W}, \mathcal{Q})$ of the graph $\mathcal{F}'$ is said to be a *non-attractive directed quasi-concave hill component* or *NA-DQCH component* of $\mathcal{F}'$ if and only if

- $\mathcal{H}$ is a DQCH;
- $\exists\, i \in \mathcal{W}$ and $j \in {}^{\text{out}}\mathcal{N}^i(\mathcal{F})$ such that $j \notin \mathcal{W}$. •

See Figure 6 in Appendix I for examples of A-DQCH and NA-DQCH components of a directed graph.

From the definition of an A-DQCH component, it is clear that if some fraction of population starts inside it, then the fraction remains there forever as there are no outgoing arcs from such a component to other components. This is the main reasoning for the nomenclature. Moreover, for every DQCH component, if the fraction of population in the said component is known apriori, we can use (4) to calculate the steady-state social utility for that population fraction. Thus, the graph $\hat{\mathcal{F}}$ (the ICRG of $\mathcal{G}$) can be partitioned into such DQCH components in order to formulate a suitable optimization problem (like in Section IV-A) for providing a lower bound on the steady-state social utility. Note that such a partition is not unique. We use the following partition to tighten the lower bound as much as possible.

Definition 4.7: (Maximal attractive component partition or MAC partition). A collection of subgraphs $\{\mathcal{H}^q = (\mathcal{W}^q, \mathcal{Q}^q)\}_{q\in[1,n]_{\mathbb{Z}}}$ is said to be a *maximal attractive component partition* or *MAC partition* of a directed graph $\mathcal{F}' = (\mathcal{V}', \mathcal{A}')$ if and only if

- $\forall q, r \in [1,n]_{\mathbb{Z}}$ such that $q \neq r$, $\mathcal{W}^q \cap \mathcal{W}^r = \varnothing$, $\mathcal{Q}^q \cap \mathcal{Q}^r = \varnothing$;
- $\bigcup_{q\in[1,n]_{\mathbb{Z}}} \mathcal{W}^q = \mathcal{V}'$, $\bigcup_{q\in[1,n]_{\mathbb{Z}}} \mathcal{Q}^q \subseteq \mathcal{A}'$;
- $\forall q \in [1,n]_{\mathbb{Z}}$, $\mathcal{H}^q$ is a DQCH component of $\mathcal{F}'$;
- $\forall q \in [1,n]_{\mathbb{Z}}$ if $\mathcal{H}^q$ is an NA-DQCH component, then $\mathcal{H}^q$ does not contain any A-DQCH component of $\mathcal{F}'$;
- $\forall q \in [1,n]_{\mathbb{Z}}$ if $\mathcal{H}^q$ is an A-DQCH component, then $\nexists \mathcal{I} \subseteq [1,n]_{\mathbb{Z}}$ such that $\overline{\mathcal{H}}^q := \left(\bigcup_{r\in\mathcal{I}\cup\{q\}} \mathcal{W}^r, \bigcup_{r\in\mathcal{I}\cup\{q\}} \mathcal{Q}^r\right)$ is an A-DQCH component. •

Definition 4.7 can be interpreted in the following way. For a MAC partition, the individual components are non-overlapping and cover the original graph. The NA-DQCH components do not contain any A-DQCH components. Finally, different components cannot be joined to create a new, larger A-DQCH component. Hence, the partition is maximally attractive. Note that a MAC partition of a directed graph always exists as a node in itself is a DQCH component of a graph. So is a combination of two neighboring nodes of the graph. Thus, a way to find a MAC partition would be to locate all the A-DQCH components of $\mathcal{F}$ and then club the remaining nodes and arcs into different NA-DQCH components. This is the main logic behind Algorithm 3 and the supporting Algorithm 4. In particular, the function `MACPartition()`, which we describe in Algorithm 3, takes a directed graph $\mathcal{F}'$ as an input and returns a MAC partition of the same.

Remark 4.8: (Computation of MAC partitions of $\hat{\mathcal{F}}$). The function `MACPartition`$(\hat{\mathcal{F}}, \mathbf{a})$ in Algorithm 3 computes a MAC partition of $\hat{\mathcal{F}}$. The function `makeQCHComp()` in Algorithm 4 aids in this process. Notice that if any directed graph is passed to `makeQCHComp()`, it returns a collection of DQCH components. This is because in Step 5, a node i with highest value of $\mathbf{a}_i$ is chosen. This definitely belongs to a DQCH component as every node in itself is a DQCH component. Then in Step 6, all nodes that have a path with quasi-concave MPDP's from this node is included into this component. Thus $(\mathcal{V}_{\text{temp}}, \mathcal{A}_{\text{temp}})$ at the end of a pass of the while loop is a DQCH by definition. The algorithm then repeats the process by considering the nodes which have not been visited in this process.

Now once such a collection of DQCH components is returned by `makeQCHComp()` to `MACPartition()` in Step 1, Algorithm 3 checks every component and removes nodes that have out-neighbors not within that component (Step 10). Thus the nodes and arcs remaining (if any) at the end (Step 17) of each pass of the for-loop forms an A-DQCH component. The nodes and arcs added to $\mathcal{V}_{\text{regroup}}$ and $\mathcal{A}_{\text{regroup}}$ in Steps 12, 13 have the property that they have outgoing arcs to some other components. Thus they are regrouped into NA-DQCH components in Step 20. Note that any NA-DQCH component formed in this process cannot contain any A-DQCH because of the aforementioned property. Thus, the partition obtained at the end of Algorithm 3 satisfies all the requirements of Definition 4.7. •

Algorithm 3: MACPartition($\mathcal{F}', \mathbf{a}$)

```
Data: $\mathcal{F}' = (\mathcal{V}', \mathcal{A}'), \mathbf{a}$
Result: MAC Partition $\mathcal{H}$
$\mathcal{H} \leftarrow$ makeQCHComp($\mathcal{F}', \mathbf{a}$)
$\mathcal{V}_{\text{regroup}} \leftarrow \varnothing$
$\mathcal{A}_{\text{regroup}} \leftarrow \varnothing$
for $\mathcal{H}^q \in \mathcal{H}$ do
                                        ▶ $\mathcal{H}^q = (\mathcal{W}^q, \mathcal{Q}^q)$
    tempVar $\leftarrow \varnothing$
    while $\mathcal{W}^q \neq$ tempVar do
        tempVar $\leftarrow \mathcal{W}^q$
        for $i \in \mathcal{W}^q$ do
            if $\exists j \in {}^{\text{out}}\mathcal{N}^i(\mathcal{F}')$ such that $j \notin \mathcal{W}^q$ then
                                        ▶ ${}^{\text{out}}\mathcal{N}^i(\mathcal{F}')$ is with respect to $\mathcal{F}'$
                $\mathcal{W}^q \leftarrow \mathcal{W}^q \setminus \{i\}$
                                        ▶ remove nodes with out-neighbors
                                          not in $\mathcal{W}^q$ and try to
                                          make $\mathcal{W}^q$ an A-DQCH
                $\mathcal{Q}^q \leftarrow \mathcal{Q}^q \setminus \{(i,k) \in \mathcal{Q}^q\} \setminus \{(k,i) \in \mathcal{Q}^q\}$
                                        ▶ remove corresponding arcs
                $\mathcal{V}_{\text{regroup}} \leftarrow \mathcal{V}_{\text{regroup}} \cup \{i\}$
                $\mathcal{A}_{\text{regroup}} \leftarrow \mathcal{A}_{\text{regroup}} \cup \{(i,k) \in \mathcal{A}'\}$
                Remove $\mathbf{a}_i$ from $\mathbf{a}$
            end
        end
    end
end
$\mathcal{F}_{\text{regroup}} \leftarrow (\mathcal{V}_{\text{regroup}}, \mathcal{A}_{\text{regroup}})$
$\mathcal{H} \leftarrow \mathcal{H} \cup$ makeQCHComp($\mathcal{F}_{\text{regroup}}, \mathbf{a}$)
                                        ▶ regroup the remaining nodes and arcs
                                          into NA-DQCH components
return: $\mathcal{H}$
```

Algorithm 4: makeQCHComp($\mathcal{F}', \mathbf{a}$)

```
Data: $\mathcal{F}' = (\mathcal{V}', \mathcal{A}'), \mathbf{a}$
Result: DQCH components
visitSet $\leftarrow \varnothing$
                                        ▶ keeps track of nodes already visited
$\mathcal{H} \leftarrow \varnothing$
while visitSet $\neq \mathcal{V}'$ do
    $i \leftarrow \arg\max(\mathbf{a})$
    $\mathcal{V}_{\text{temp}} \leftarrow \{i\}$
                                        ▶ node with highest MPDP is
                                          definitely in a QCH
    $\mathcal{V}_{\text{temp}} \leftarrow \mathcal{V}_{\text{temp}} \cup \{j \in \mathcal{V}' \mid \exists$ a path with
        quasi-concave MPDP's between $j$ and $i$ in $\mathcal{F}'\}$
                                        ▶ these consider paths in the
                                          undirected sense
    $\mathcal{A}_{\text{temp}} \leftarrow \{(i,j) \in \mathcal{A}' \mid i,j \in \mathcal{V}_{\text{temp}}\}$
    visitSet $\leftarrow$ visitSet $\cup \mathcal{V}_{\text{temp}}$
    Remove indices $\{i \in$ visitSet$\}$ from $\mathbf{a}$
    $\mathcal{H} \leftarrow \mathcal{H} \cup \{(\mathcal{V}_{\text{temp}}, \mathcal{A}_{\text{temp}})\}$
end
return: $\mathcal{H}$
```

Using such a partition, we can create a super graph of $\hat{\mathcal{F}}$ (the ICRG of $\mathcal{G}$) in order to find a lower bound on the steady-state social utility of the dynamics. This is also useful as it reduces the number of variables (significantly in some cases) as we can group multiple nodes into a super node and consider the super node as a whole rather than considering the individual nodes that constitute it.

Definition 4.9: (Maximal attractive component super graph or MAC-SG). Suppose $\{\mathcal{H}^q = (\mathcal{W}^q, \mathcal{Q}^q)\}_{q\in[1,n]_{\mathbb{Z}}}$ is a MAC partition of a directed graph $\mathcal{F}' = (\mathcal{V}', \mathcal{A}')$. Construct a graph $\Gamma := (\Lambda, \Pi)$ with the following property:

- $\Lambda = [1, n]_{\mathbb{Z}}$;
- $(q, r) \in \Pi$ if and only if $\exists\ i \in \mathcal{W}^q$ and $j \in \mathcal{W}^r$ such that $(i, j) \in \mathcal{A}'$.

Such a graph Γ is called a *Maximal Attractive Component Super Graph* or *MAC-SG* of the MAC partition $\{\mathcal{H}^q = (\mathcal{W}^q, \mathcal{Q}^q)\}_{p\in[1,n]_{\mathbb{Z}}}$ of $\mathcal{F}'$. The q's are called super nodes.

The function MACSG() takes in a MAC partition of $\mathcal{F}'$ and returns the corresponding MAC-SG. •

See Figure 7 in Appendix I for example of a MAC partition and corresponding MAC-SG of a directed graph.

Let $\Gamma := (\Lambda, \Pi)$ be such a MAC-SG of a MAC partition of $\hat{\mathcal{F}}$ (the ICRG of $\mathcal{G}$). Similar to the nodes, for a super node $q \in \Lambda$, we define the set of in-reachable super nodes of q as ${}^{\text{in}}\mathcal{R}^q := \{r \in \Lambda \,|\, \exists$ a directed path from r to q in $\Gamma\} \cup \{q\}$ and the set of out-reachable super nodes of q as ${}^{\text{out}}\mathcal{R}^q := \{r \in \Lambda \,|\, \exists$ a directed path from q to r in $\Gamma\} \cup \{q\}$. We then let $\overline{\rho}_{qr}$ denote the fraction of population moving from super node $q \in \Lambda$ to $r \in \Lambda$ and $\overline{\rho}$ be the vector that accumulates all such $\overline{\rho}_{qr}$ into a vector. Of course such a movement is only allowed between nodes if there is a directed path between them. Moreover, the total fraction of population that moves out of a super node cannot be more than the initial fraction that starts off in that node. Thus,

$$\overline{\rho}_{qr} \geq 0, \quad \forall r \in {}^{\text{out}}\mathcal{R}^q, \forall q \in \Lambda, \tag{9a}$$

$$\sum_{r\in {}^{\text{out}}\mathcal{R}^q} \overline{\rho}_{qr} = \sum_{j\in\mathcal{W}^q} \mathbf{x}_j^0, \quad \forall q \in \Lambda\,. \tag{9b}$$

Now, if we allow the entire population to fit in every super node, then we might end up with a conservative lower bound. To compute a more realistic lower bound, the fact that some nodes will not contain any population fraction in the steady-state must be taken into account. We formally define such nodes next and then provide a result to identify such nodes.

Definition 4.10: (Eventually empty nodes). Let the evolution of $\mathbf{x}$ be governed by a Nash convergent dynamics from an initial condition $\mathbf{x}^0$. Let $\mathcal{L}^+$ be the positive limit set of the trajectory. Then $i \in \mathcal{V}$ is said to be an eventually empty node if and only if $\overline{\mathbf{x}}_i = 0$, $\forall \overline{\mathbf{x}} \in \mathcal{L}^+$. •

Lemma 4.11: (Sufficient condition for being eventually empty). Let the evolution of $\mathbf{x}$ be governed by (3) with Assumptions **(A2)**, **(A3)** and **(A5)**. Let $\mathbf{x}^0 \in \mathcal{S}_\rho^{|\mathcal{V}|}$ and let $\hat{\mathcal{F}} = (\hat{\mathcal{V}}, \hat{\mathcal{A}})$ be an ICRG of $\mathcal{G} = (\mathcal{V}, \mathcal{E})$. For a node $i \in \hat{\mathcal{V}}$, if $\exists\, j \in \mathcal{N}^i$ such that $(i, j) \in \hat{\mathcal{A}}$ and $(j, i) \notin \hat{\mathcal{A}}$, then i is an eventually empty node. •

A proof of this is provided in Appendix II-C.2. Thus, if a super node contains an eventually empty node, there exists an inherent bound on the fraction of population that can stay in that super node in the steady-state state as this state is a Nash equilibrium. We discuss this in the following result.

Lemma 4.12: (Upper bound on population fraction in super nodes). Let the evolution of $\mathbf{x}$ be governed by (3) with Assumptions **(A2)**, **(A3)** and **(A5)**. Suppose $\mathbf{x}^0$ is the initial condition and $\hat{\mathcal{F}}$ is an ICRG of $\mathcal{G}$. Let $\{\mathcal{H}^q = (\mathcal{W}^q, \mathcal{Q}^q)\}_{q\in[1,n]_{\mathbb{Z}}}$ be a MAC partition of $\hat{\mathcal{F}}$ and let $\Gamma = (\Lambda, \Pi)$ be the corresponding MAC-SG. Let $\mathcal{L}^+$ be the positive limit set of the trajectories. For a super node $q \in \Lambda$, let the set of eventually empty nodes in q be denoted by $\mathcal{M}^q := \{i \in \mathcal{W}^q \,|\, i \text{ is eventually empty}\}$. Let

$$\mathbf{a}_q^{\max} := \max_{i\in\mathcal{M}^q} \mathbf{a}_i, \quad \text{if } \mathcal{M}^q \neq \varnothing\,, \tag{10}$$

and finally, let

$$\rho_q^{\max} := \begin{cases} 0, & \text{if } \mathcal{M}^q = \mathcal{W}^q \\ \displaystyle\sum_{i\in\mathcal{W}^q\setminus\mathcal{M}^q} u_i^{-1}\left(\mathbf{a}_q^{\max}\right), & \text{if } \mathcal{W}^q \supset \mathcal{M}^q \neq \varnothing, \\ 1, & \text{if } \mathcal{M}^q = \varnothing\,. \end{cases} \tag{11}$$

Then, $\forall\, \overline{\mathbf{x}} \in \mathcal{L}^+$

$$\sum_{i\in\mathcal{W}^q} \overline{\mathbf{x}}_i \leq \rho_q^{\max}, \;\; \forall\, q \in \Lambda\,. \tag{12}$$

•

We present a proof in Appendix II-C.3.

Recall that $f_{\mathcal{V}'}(\rho)$ is the solution of the optimization problem $\mathbf{P}_1(\mathcal{V}', \rho)$ in (4). The optimum of the following optimization problem then provides a lower bound on the steady-state social utility.

$$\begin{aligned} \mathbf{P}_5 : \quad & U_{\min} := \min_{\xi, \overline{\rho}} \sum_{q\in\Lambda} f_{\mathcal{W}^q}\left(\xi_q\right) \\ & \text{s.t. } \xi_q = \sum_{r\in{}^{\text{in}}\mathcal{R}^q} \overline{\rho}_{rq}, \forall q \in \Lambda, \;(9), \;\xi_q \leq \rho_q^{\max}, \forall q \in \Lambda\,. \end{aligned}$$

The following lemma, proof of which is given in Appendix II-C.4 shows concavity of the cost function in $\mathbf{P}_5$.

Lemma 4.13: (Concavity of cost function of $\boldsymbol{P}_5$). Consider a fixed $\mathcal{V}'$ and the function $f_{\mathcal{V}'}(\rho)$ which is the optimum of $\mathbf{P}_1(\mathcal{V}', \rho)$ in (4). Then $f_{\mathcal{V}'}(\rho)$ is concave in $\rho \geq 0$. •

The constraints set of $\mathbf{P}_5$ is a polyhedron. Thus it is a well known fact that the global optimum will occur at an extreme point. Any standard method such as [18]–[20] can be used to solve this problem.

The main sequence of steps, required to compute a lower bound on the steady-state social utility, described in this section is listed in Algorithm 5 and the result regarding the same is stated to conclude the section.

Theorem 4.14: (Lower bound on steady-state social utility for SSD, NBRD and NRPM). Let $\mathbf{x}^0 \in \mathcal{S}_\rho^{|\mathcal{V}|}$ and the evolution of $\mathbf{x}$ be governed by (3) with Assumptions **(A2) - (A5)** . Then the steady-state social utility from the initial condition $\mathbf{x}^0$ is lower bounded by $U_{\min}$, *i.e* $U_{\min} \leq U_{\text{ss}}(\mathbf{x}^0)$.

Further if the solution $\mathbf{x}(t)$ of (3) is such that $U(\mathbf{x}(t)) \geq U(\mathbf{x}^0)$, $\forall t \geq 0$, then $\max\{U_{\min}, U(\mathbf{x}^0)\} \leq U_{\text{ss}}(\mathbf{x}^0)$. •

A proof of this is presented in Appendix II-C.5.

Algorithm 5: Compute lower bound for steady-state social utility

```
Data: $\mathbf{x}^0, \mathcal{F}$
Result: $U_{\min}$
$\hat{\mathcal{F}} \leftarrow$ reduceGraph($\mathcal{F}, \mathbf{x}^0$)
$\mathcal{H} \leftarrow$ MACPartition($\hat{\mathcal{F}}$)
        ▶ individual components are $\mathcal{H}^q = (\mathcal{W}^q, \mathcal{Q}^q)$
$\Gamma \leftarrow$ MACSG($\mathcal{H}$)                    ▶ $\Gamma = (\Lambda, \Pi)$
$U_{\min} \leftarrow$ solution of $\mathbf{P}_5$
```

V. Simulations and Analysis

In this section, we highlight some properties of SSD, NBRD and NRPM and illustrate some results stated in Parts I and II using some simulations. We used CVXPY [21], [22] for solving the optimization problems. We performed all simulations in a python3 programming language environment on a standard laptop with intel 10th generation Core i5 processor.

A. Myopic Coordination can be Worse than Myopic Selfish Behavior

Even though SSD, NBRD and NRPM converge asymptotically to the set of Nash equilibria, they may not converge to the same state in general. Further, even though these dynamics display increasing levels of coordination among the agents, it is not always true that NBRD performs better than SSD nor that NRPM performs better than NBRD. This is because these are still essentially network restricted gradient ascent dynamics with myopic agents. In this subsection we illustrate a situation where the act of coordination does not result in better social utility. For this subsection we assume the cumulative payoff functions to be of the form $p_i(\mathbf{x}_i) := -0.5\mathbf{x}_i^2 - \mathbf{a}_i\mathbf{x}_i$. This is the uniform water tank model presented in [17].

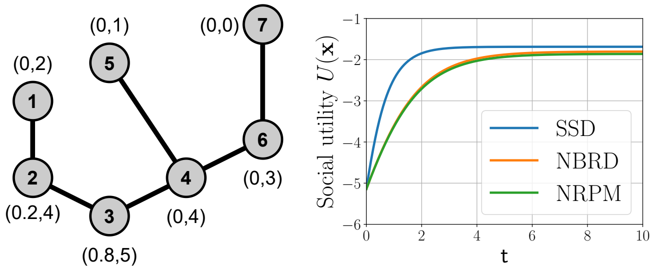

(a) (b)

Fig. 1: SSD outperforms NBRD, which outperforms NRPM. (a) Graph, initial state and MPDP's. The tuple $(.,.)$ near each node i represents $(\mathbf{x}_i^0, \mathbf{a}_i)$. (b) Evolution of social utility.

1) SSD outperforms NBRD which in turn outperforms NRPM:

Consider the graph, initial state and MPDP's in Figure 1(a). In case of NRPM, unlike SSD and NBRD, the population is aware of the choice revision of the fraction in node 2 to node 1. Thus under NRPM, more population moves from node 3 to node 2, than under SSD and NBRD, in order to instantaneously maximize the social utility. But, in the longterm, more population is able to access the more lucrative nodes 5 and 7 in case of SSD and NBRD than NRPM. Now, when the population reaches node 4, all the agents find it instantaneously optimal under NBRD and NRPM to move to node 5. Hence, they completely miss out on the best payoff in node 7. SSD on the other hand sends some non-zero population fraction from node 4 to nodes 5 and 6. Thus it attains the best steady state social utility. This is seen in the simulation results in Figure 1(b).

B. Evolution on a Quasi Concave Hill

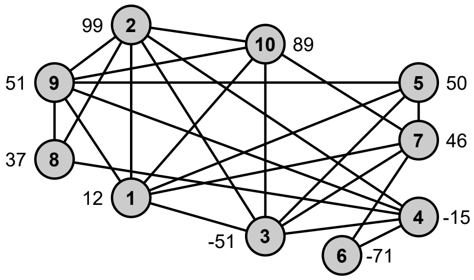

Fig. 2: 10-node QCH for simulation. The MPDP's of each node are mentioned near it. The nodes are positioned in order of increasing MPDP's in the vertical direction.

In this section, we verify the results provided in Section III. We first studied the evolution of the population on the 10-node QCH shown in Figure 2 from an initial condition $\mathbf{x}^0 = 0.1 \times \mathbf{1}$. The simulation results are shown in Figure 3. It can be seen that the population concentrates to nodes $2, 5, 9$ and 10 which have MPDP's greater than the rest of the nodes.

We also randomly selected 5 QCH's with 10 nodes and for each QCH we ran SSD, NBRD and NRPM for 10 uniformly randomly selected initial conditions from $\mathcal{S}_1^{10}$. For each graph, $p(.)$'s were randomly chosen from a class of strictly concave polynomials of degree 2, 4 or 6. We then compared the steady-state utility for all three dynamics with the solution of $\mathbf{P}_1$. The maximum absolute relative error was 9.44×10^{-5}.

C. Bounds on Steady-State Social Utility

1) General Example: Here we consider an 18 node graph and quadratic cumulative payoff functions and verify the upper and lower bounds on the steady-state social utility. The graph structure $\mathcal{G}$ and cumulative payoff function details are provided in Figure 4(a). Initial population is distributed between nodes $4, 10, 17$ and 18 as $\mathbf{x}_4^0 = \mathbf{x}_{10}^0 = 0.1$, $\mathbf{x}_{17}^0 = 0.3$, $\mathbf{x}_{18}^0 = 0.5$ and $\mathbf{x}_i^0 = 0$, $\forall i \in [1, 18]_{\mathbb{Z}} \setminus \{4, 10, 17, 18\}$. The corresponding ICRG $\hat{\mathcal{F}}$ is provided in Figure 4(b). Note that $\hat{\mathcal{F}}$ has only 17 nodes and not 18 (node 7 has been removed). The only bi-directional arc in $\hat{\mathcal{F}}$ is between nodes 1 and 4. Rest of the arcs are all uni-directional. Thus there is over 50% reduction of δ_{ij} variables from $\mathcal{G}$ to $\hat{\mathcal{F}}$. The A-DQCH components are made up of the node sets $\{2\}, \{8\}, \{9, 14, 17\}, \{10\}, \{16\}$ and corresponding arcs. The NA-DQCH components are made up of the node sets $\{1, 3, 4, 5, 6, 11, 12, 15\}, \{13\}, \{18\}$ and corresponding arcs. To compute the upper and lower bounds the total time taken was ≈ 3.48 sec.

Social utility order	Rate	Social utility order	Rate
$U_{\text{ss}}^1 \geq U_{\text{ss}}^2 \geq U_{\text{ss}}^3$	22.8%	$U_{\text{ss}}^2 \geq U_{\text{ss}}^3 \geq U_{\text{ss}}^1$	17.2%
$U_{\text{ss}}^1 \geq U_{\text{ss}}^3 \geq U_{\text{ss}}^2$	18.6%	$U_{\text{ss}}^3 \geq U_{\text{ss}}^1 \geq U_{\text{ss}}^2$	4.8%
$U_{\text{ss}}^2 \geq U_{\text{ss}}^1 \geq U_{\text{ss}}^3$	0.8 %	$U_{\text{ss}}^3 \geq U_{\text{ss}}^2 \geq U_{\text{ss}}^1$	35.8%

TABLE I: Trends in steady-state social utility of SSD, NBRD and NRPM. Steady state social utility of SSD, NBRD and NRPM are respectively denoted by $U_{\text{ss}}^1, U_{\text{ss}}^2$ and U_{ss}^3.

The simulation results are provided in Figures 4(c) - 4(f). The time axis in each of these diagrams is represented as a log scale, *i.e.* each tick on the horizontal axis represents $\log(k^{-1}t + 1)$ rather than t (the value of k is given in Figure 4). This is done to magnify the initial time frame where the main redistribution occurs and shrink the later time frame. The average time taken to solve the optimization problems for NBRD and NRPM were ≈ 0.32 sec and ≈ 0.16 sec respectively. The total time required to complete the simulations for SSD, NBRD and NRPM were ≈ 108.43 sec, $\approx 3.19 \times 10^4$ sec and $\approx 1.6 \times 10^4$ sec respectively. The upper and lower bounds obtained were -3.17 and -7.58 respectively while the actual steady-state social utility for SSD, NBRD and NRPM were -5.16, -5.01 and -4.17 respectively.

2) Performance of Bounds with Varying Graph Sparsity: We studied the performance of the bounds by varying the graph sparsity. We chose 5 cases where the probability of an edge between two nodes takes values $0.1, 0.2, 0.3, 0.4$ and 0.5. Then for each probability value, we randomly selected 10 connected graphs with 10 nodes and for each graph we ran SSD, NBRD and NRPM for 10 uniformly randomly selected initial conditions from $\mathcal{S}_1^{10}$. For each graph, $p(.)$'s were randomly chosen from a class of strictly concave polynomials of degree 2, 4 or 6. We then compared the steady state utility for all three dynamics with the bounds U_{max}, U_{min} and $\max\{U_{\text{min}}, U(\mathbf{x}^0)\}$. The data from these 500 simulations is shown in Figure 5. We also provide the percentage of sims a particular ordering of the steady-state social utility of SSD, NBRD and NRPM appeared in these 500 sample simulations in Table I. We provide an intuitive reasoning behind this data in Remark 5.1.

Remark 5.1: (Intuitive Reasoning behind data in Table I). From Table I, it is visible that in majority of the sims NRPM performs better than NBRD and NBRD performs better than SSD. This is to be expected as SSD, NBRD and NRPM show an increasing level of coordination. However, surprisingly, the reverse ordering takes the second position. This means that quite often myopic coordination is worse than myopic selfishness (see Section V-A). It should also be noted that very few times SSD ends up between NBRD and NRPM. We believe that this happens because both NBRD and NRPM have similar optimization problems at their core; whereas SSD redistributes the population selfishly based on what is available. Further analysis needs to be done to rigorously talk about the ordering percentages. •

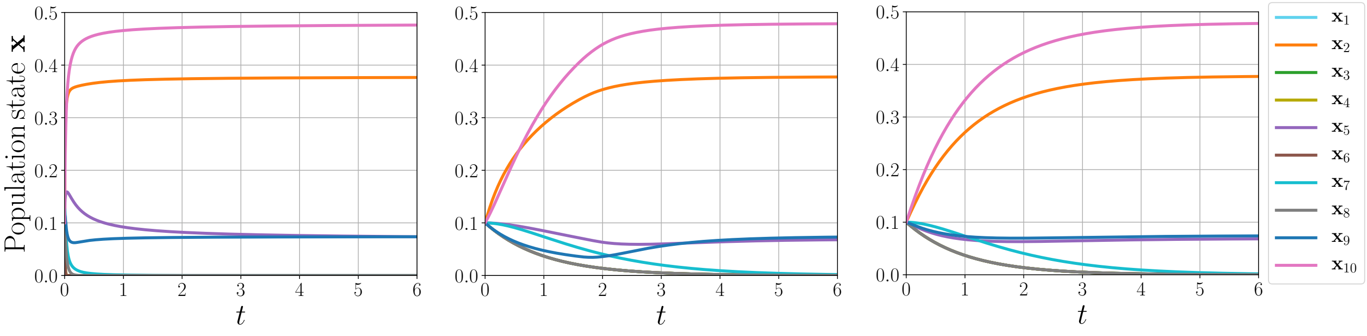

(a) (b) (c)

Fig. 3: Evolution of population state on a QCH. The plots share a common label and a common legend. (a) Evolution of population state under SSD. (b) Evolution of population state under NBRD. (c) Evolution of population state under NRPM.

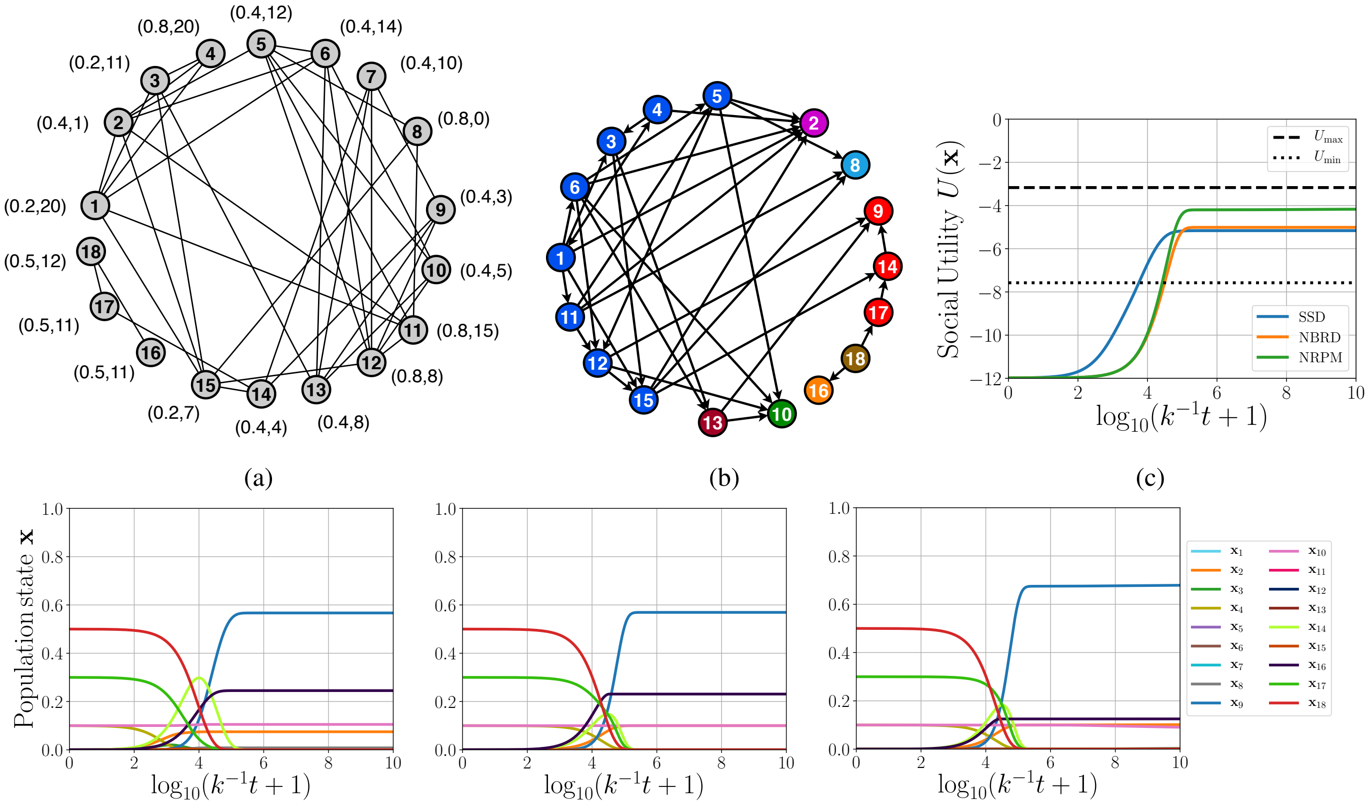

(a) (b) (c)

(d) (e) (f)

Fig. 4: Simulation with $p_i(\mathbf{x}_i) := -\alpha_i\,\mathbf{x}_i^2 - \beta_i\,\mathbf{x}_i$. The last three plots share a common label and a common legend. Here $k \approx 5 \times 10^{-5}$. (a) Graph structure with 18 nodes. The tuple (.,.) around each node i represents (α_i, β_i). (b) Corresponding ICRG. Nodes in same D-QCH components have same color and have been grouped together. Nodes in different D-QCH components are colored differently. (c) Evolution of social utility and bounds on steady-state social utility. (d) Evolution of population state under SSD. (e) Evolution of population state under NBRD. (f) Evolution of population state under NRPM.

VI. Conclusion

We provided sufficient conditions on the network under which there exists a unique Nash equilibrium for the stratified population game. We also provided algorithms to reduce the graph using the initial condition without affecting the population evolution. We then provided algorithms to partition the reduced graph and utilized the conditions for unique Nash equilibrium to provide upper and lower bounds on the steady-state social utility for SSD, NBRD and NRPM.

Future work includes utilizing the dynamics to further reduce the graph and refine the bounds on the steady-state social utility. We would also like to extend the ideas further

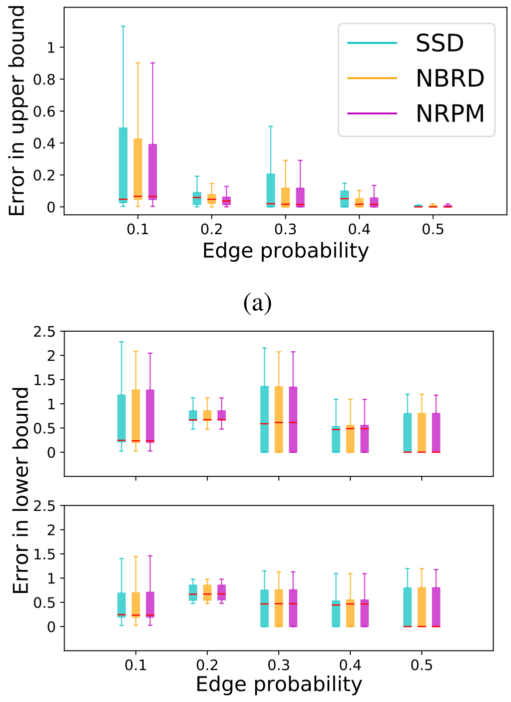

(a)

(b)

Fig. 5: Absolute relative error of bounds. The plots share a common legend. (a) Absolute relative error of upper bound $U_{\max}$. (b) Absolute relative error of lower bounds. Upper plot considers $U_{\min}$ and lower plot considers $\max\{U_{\min}, U(\mathbf{x}^0)\}$.

to compute conditions under which the bounds coincide and utilize this knowledge to compute the steady-state state.

References

[1] N. Mandal and P. Tallapragada, "Dynamics of a stratified population of optimum seeking agents on a network–Part I: Modeling and convergence analysis," *arXiv preprint arXiv:2012.12599*, 2020.

[2] W. H. Sandholm, *Population games and evolutionary dynamics*. MIT press, 2010.

[3] N. Quijano, C. Ocampo-Martinez, J. Barreiro-Gomez, G. Obando, A. Pantoja, and E. Mojica-Nava, "The role of population games and evolutionary dynamics in distributed control systems: The advantages of evolutionary game theory," *IEEE Control Systems Magazine*, vol. 37, no. 1, pp. 70–97, 2017.

[4] J. Barreiro-Gomez, G. Obando, and N. Quijano, "Distributed population dynamics: Optimization and control applications," *IEEE Transactions on Systems, Man, and Cybernetics: Systems*, vol. 47, no. 2, pp. 304–314, 2016.

[5] J. Martinez-Piazuelo, G. Diaz-Garcia, N. Quijano, and L. F. Giraldo, "Distributed formation control of mobile robots using discrete-time distributed population dynamics," *IFAC-PapersOnLine*, vol. 53, no. 2, pp. 3131–3136, 2020.

[6] E. Lieberman, C. Hauert, and M. A. Nowak, "Evolutionary dynamics on graphs," *Nature*, vol. 433, no. 7023, p. 312, 2005.

[7] K. Pattni, M. Broom, J. Rychtář, and L. J. Silvers, "Evolutionary graph theory revisited: When is an evolutionary process equivalent to the Moran process?" *Proceedings of the Royal Society A: Mathematical, Physical and Engineering Sciences*, vol. 471, no. 2182, p. 20150334, 2015.

[8] L.-M. Hofmann, N. Chakraborty, and K. Sycara, "The evolution of cooperation in self-interested agent societies: A critical study," in *The 10th International Conference on Autonomous Agents and Multiagent Systems-Volume 2*, 2011, pp. 685–692.

[9] B. Allen and M. A. Nowak, "Games on graphs," *EMS surveys in mathematical sciences*, vol. 1, no. 1, pp. 113–151, 2014.

[10] B. Allen, G. Lippner, Y.-T. Chen, B. Fotouhi, N. Momeni, S.-T. Yau, and M. A. Nowak, "Evolutionary dynamics on any population structure," *Nature*, vol. 544, no. 7649, pp. 227–230, 2017.

[11] G. Como, F. Fagnani, and L. Zino, "On imitation dynamics for potential population games over networks with community patterns," in *21st IFAC World Congress*, 2020.

[12] J. Barreiro-Gomez and H. Tembine, "Constrained evolutionary games by using a mixture of imitation dynamics," *Automatica*, vol. 97, pp. 254–262, 2018.

[13] ——, "Distributed evolutionary games reaching power indexes: Navigability in a social network of smart objects," in *2018 European Control Conference (ECC)*. IEEE, 2018, pp. 1062–1067.

[14] J. Barreiro-Gomez, G. Obando, A. Pantoja, and H. Tembine, "Heterogeneous multi-population evolutionary dynamics with migration constraints," *IFAC-PapersOnLine*, vol. 53, no. 2, pp. 16 852–16 857, 2020.

[15] D. Gadjov and L. Pavel, "A passivity-based approach to nash equilibrium seeking over networks," *IEEE Transactions on Automatic Control*, vol. 64, no. 3, pp. 1077–1092, 2018.

[16] M. Bianchi and S. Grammatico, "Continuous-time fully distributed generalized nash equilibrium seeking for multi-integrator agents," *Automatica*, vol. 129, p. 109660, 2021.

[17] N. Mandal and P. Tallapragada, "Evolution of a population of selfish agents on a network," *IFAC-PapersOnLine*, vol. 53, no. 2, pp. 3385–3390, 2020.

[18] M. E. Dyer and L. G. Proll, "An algorithm for determining all extreme points of a convex polytope," *Mathematical Programming*, vol. 12, no. 1, pp. 81–96, 1977.

[19] T. Matheiss and D. S. Rubin, "A survey and comparison of methods for finding all vertices of convex polyhedral sets," *Mathematics of operations research*, vol. 5, no. 2, pp. 167–185, 1980.

[20] H. P. Benson, "A finite algorithm for concave minimization over a polyhedron," *Naval Research Logistics Quarterly*, vol. 32, no. 1, pp. 165–177, 1985.

[21] S. Diamond and S. Boyd, "CVXPY: A Python-embedded modeling language for convex optimization," *Journal of Machine Learning Research*, vol. 17, no. 83, pp. 1–5, 2016.

[22] A. Agrawal, R. Verschueren, S. Diamond, and S. Boyd, "A rewriting system for convex optimization problems," *Journal of Control and Decision*, vol. 5, no. 1, pp. 42–60, 2018.

[23] S. Boyd and L. Vandenberghe, *Convex optimization*. Cambridge university press, 2004.

Appendix I
Examples for Section IV

The nodes of the graphs in Figures 6 and 7-(a) are arranged in a way that the MPDP's or $\mathbf{a}_i$'s increase in the vertical direction. This makes it easier to verify the definitions.

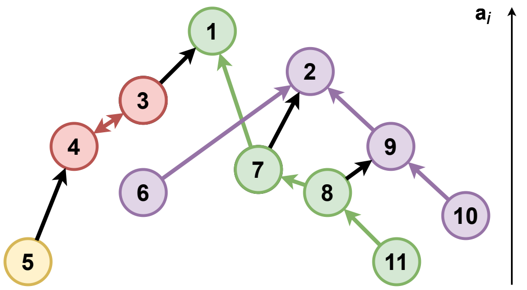

Fig. 6: Example of A-DQCH and NA-DQCH components of a directed graph. Different components are given in different colors. A-DQCH component is made up of the nodes $\{2, 6, 9, 10\}$. There are three NA-DQCH components, with the node sets $\{1, 7, 8, 11\}$, $\{3, 4\}$ and $\{5\}$, respectively.

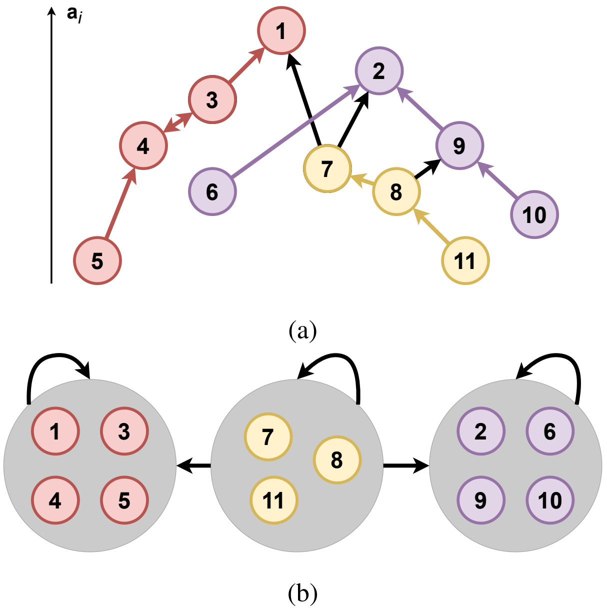

Fig. 7: MAC partition and MAC-SG (a) A MAC partition of the directed graph in Figure 6. Different components are in different colors. (b) Corresponding MAC-SG.

Appendix II
Proofs of Results

A. Proof of Lemma 2.2

The fact that SSD, NBRD and NRPM satisfy Assumptions **(A2)** - **(A4)** can be found in the results in [1]. Positive invariance of $\mathcal{S}_\rho^{|\mathcal{V}|}$ follows form the fact that all the three dynamics are flow balanced dynamics. The rest follows from Remark 4.1, Theorem 4.2, Theorem 5.5, Lemma 6.8 and Theorem 6.9 in [1].

Next, we prove that SSD and NBRD satisfy Assumption **(A5)**. Since $u_i(.)$ is strictly decreasing $\forall i \in \mathcal{V}$, we can say that $\forall (i,j) \in \mathcal{A}$ such that $u_i(\theta_i) \ge u_j(0)$

$$u_i(\mathbf{x}_i) \ge u_i(\theta_i) \ge u_j(0) \ge u_j(\mathbf{x}_j), \quad \forall \mathbf{x}_i \in [0,\theta_i],\ \forall \mathbf{x}_j \ge 0.$$

Thus, (6) follows from strong positive correlation of SSD and NBRD with $u(.)$ as described in [1].

Note that for NRPM, $\mathbf{F}_i(\mathbf{x}) + \mathbf{x} = \mathbf{z}^*(\mathbf{x})$, where $\mathbf{z}^*$ comes from an optimizer of $\mathbf{P}_3$. Also recall that, if $(\mathbf{z}^*, \mathbf{d}^*)$ is an optimizer of $\mathbf{P}_3$, then

$$u_j(\mathbf{z}_j^*) \ge u_i(\mathbf{z}_i^*),\ \forall j \in \mathcal{N}^i \text{ s.t. } \mathbf{d}_{ij}^* > 0\,. \tag{13}$$

Moreover, $(\mathbf{z}^*, \mathbf{d}^*)$ satisfies the feasibility constraints,

$$\mathbf{z}_i^* = \mathbf{x}_i + \sum_{j \in \mathcal{N}^i} (\mathbf{d}_{ji}^* - \mathbf{d}_{ij}^*),\ \forall\, i \in \mathcal{V}, \tag{14a}$$

$$\sum_{j \in \mathcal{N}^i} \mathbf{d}_{ij}^* = \mathbf{x}_i,\ \forall\, i \in \mathcal{V}, \tag{14b}$$

$$\mathbf{d}_{ij}^* \ge 0,\ \forall\, (i,j) \in \overline{\mathcal{A}} := \mathcal{A} \cup \{(i,i) \mid i \in \mathcal{V}\}. \tag{14c}$$

Now, we prove Assumption **(A5)** for NRPM by contradiction. Suppose $\exists \mathbf{x} \in \mathcal{S}_\rho^{|\mathcal{V}|}$ with $\mathbf{x}_i, \mathbf{z}_i^*(\mathbf{x}) \in [0,\theta_i]$ and $(i,j) \in \mathcal{A}$ such that $u_i(\theta_i) \ge u_j(0)$ but $\mathbf{d}_{ij}^* > 0$ for some $\mathbf{d}^*$ that optimizes $\mathbf{P}_3$. Then by (13), we get

$$u_i(\theta) \le u_i(\mathbf{z}_i^*) \le u_j(\mathbf{z}_j^*) < u_j(0)\,.$$

The last strict inequality can be obtained by combining the feasibility constraints (14a) for j, (14b) and (14c) of $\mathbf{P}_3$; along with the assumption that $\mathbf{d}_{ij}^* > 0$. But this is a contradiction and hence **(A5)** must hold for NRPM. ■

B. Proof of Results on Unique Nash Equilibrium

1) Proof of Lemma 3.3: (By contradiction) Suppose $\exists\, k \in [1,n]_{\mathbb{Z}}$, $p \in [1, k-1]_{\mathbb{Z}}$ and $q \in [k+1, n]_{\mathbb{Z}}$ such that $\mathbf{a}_{\pi(p)} > \mathbf{a}_{\pi(p+1)}$ and $\mathbf{a}_{\pi(q-1)} < \mathbf{a}_{\pi(q)}$. But $\pi(p), \pi(q) \in \mathcal{P}(i,j)$ which is a path of quasi-concave MPDP's and one of the previous inequalities violates the condition that $\forall\, r \in [p,q]_{\mathbb{Z}}$, $\mathbf{a}_{\pi(r)} \ge \min\{\mathbf{a}_{\pi(p)}, \mathbf{a}_{\pi(q)}\}$. This is a contradiction and hence the assumption was incorrect. ■

2) Proof of Lemma 3.5: Choose any $i, j \in \operatorname{supp}(\mathbf{x})$ and let $\mathcal{P}(i,j)$ be a path between i and j with quasi-concave MPDP's. Existence of such a path is guaranteed as the graph $\mathcal{G}$ is a QCH. Let $\pi(k) := \mathcal{P}_k(i,j)$. As $\pi(k) \in \mathcal{P}(i,j)$, by Lemma 3.3 $\mathbf{a}_i \le \mathbf{a}_{\pi(2)} \le \cdots \mathbf{a}_{\pi(k)}$ or $\mathbf{a}_{\pi(k)} \ge \cdots \ge \mathbf{a}_{\pi(n-1)} \ge \mathbf{a}_j$. Without loss of generality, suppose that $\mathbf{a}_i \le \mathbf{a}_{\pi(2)} \le \cdots \mathbf{a}_{\pi(k)}$.

Now, consider the nodes $\pi(1) = i$ and $\pi(2)$. As $\mathbf{x}_i > 0$ and $\mathbf{a}_i \le \mathbf{a}_{\pi(2)}$, we have

$$u_{\pi(2)}(0) \ge u_i(0) > u_i(\mathbf{x}_i) \ge u_{\pi(2)}(\mathbf{x}_{\pi(2)}),$$

where we have used the fact that $u_k(.)$ is a strictly decreasing function $\forall\, k$, which implies $u_k(0) > u_k(y)$ iff $y > 0$. Further, the last inequality comes from the fact that $\mathbf{x} \in \mathcal{NE}_\rho^{|\mathcal{V}|}$. Collapsing the intermediate inequalities, we thus have $u_{\pi(2)}(0) > u_{\pi(2)}(\mathbf{x}_{\pi(2)})$, which again implies $\mathbf{x}_{\pi(2)} > 0$. Now, repeating this argument for every pair of nodes $(\pi(r), \pi(r+1))$ for $r \in \{1, \ldots k-1\}$, we conclude that $\mathbf{x}_{\pi(k)} > 0$, that is $\pi(k) \in \operatorname{supp}(\mathbf{x})$.

Thus, $\forall\, \pi(k) \in \mathcal{P}(i,j)$, $\pi(k) \in \operatorname{supp}(\mathbf{x})$. Then as $\mathbf{x} \in \mathcal{NE}_\rho^{|\mathcal{V}|}$, $u_{\pi(k)}(\mathbf{x}_{\pi(k)}) = u_{\pi(l)}(\mathbf{x}_{\pi(l)})\ \forall\, \pi(k), \pi(l) \in \mathcal{P}(i,j)$. Thus $u_i(\mathbf{x}_i) = u_j(\mathbf{x}_j)$. As i and j were chosen arbitrarily, the proof of the lemma is complete. ■

3) Proof of Theorem 3.6: First note that $U(\mathbf{x})$ is a strictly concave function in $\mathbf{x}$ and $\mathbf{P}_1$ is always feasible as $\mathcal{S}_\rho^{|\mathcal{V}|}$ is non-empty. Also $\mathbf{P}_1$ is a strictly convex program and hence has a unique optimizer [23]. Thus, it suffices to show that if $\mathbf{x} \in \mathcal{NE}_\rho^{|\mathcal{V}|}$ then $\mathbf{x}$ also optimizes $\mathbf{P}_1$.

If $\rho = 0$ then the result is trivially true. So, now suppose $\rho > 0$. The Lagrangian for $\mathbf{P}_1$ can be written as

$$L_1 = \sum_{i \in \mathcal{V}} p_i(\mathbf{x}_i) - \lambda \left(\sum_{i \in \mathcal{V}} \mathbf{x}_i - \rho \right) + \sum_{i \in \mathcal{V}} \mu_i \mathbf{x}_i,$$

where λ and $\{\mu_i \ge 0\}_{i \in \mathcal{V}}$ are the Lagrange multipliers. The KKT conditions for $\mathbf{P}_1$ include

$$u_i(\mathbf{x}_i) - \lambda + \mu_i = 0,\ \forall i \in \mathcal{V}, \tag{15a}$$

$$\mu_i \mathbf{x}_i = 0,\ \forall i \in \mathcal{V}\,. \tag{15b}$$

Now, let $\mathbf{x} \in \mathcal{NE}_\rho^{|\mathcal{V}|}$. Since the graph is a QCH, we know from Lemma 3.5 that

$$u_i(\mathbf{x}_i) = H, \quad \forall\, i \in \operatorname{supp}(\mathbf{x}), \tag{16}$$

for some H. Clearly, if $\rho > 0$, problem $\mathbf{P}_1$ satisfies Slater's condition. Thus, we will show that $\mathbf{x} \in \mathcal{NE}_\rho^{|\mathcal{V}|}$ is the unique optimizer of $\mathbf{P}_1$ by showing that for $\mathbf{x}$ there exist Lagrange multipliers that satisfy (15) and the feasibility constraints. As $\mathbf{x} \in \mathcal{NE}_\rho^{|\mathcal{V}|}$, $\mathbf{x}$ is a feasible solution for $\mathbf{P}_1$. Now, we set

$$\lambda^* = H, \quad \mu_i^* = 0, \ \forall i \in \operatorname{supp}(\mathbf{x}),$$
$$\mu_j^* = H - u_j(0), \ \forall j \notin \operatorname{supp}(\mathbf{x}).$$

As $\mathbf{x} \in \mathcal{NE}_\rho^{|\mathcal{V}|}$, we can say from (16) that $\mu_j^* \geq 0$, $\forall j \notin \operatorname{supp}(\mathbf{x})$. Thus for each $i \in \mathcal{V}$, $\mu_i^* \geq 0$ and satisfies (15b). Also, we can directly verify that $(\mathbf{x}, \lambda^*, \mu^*)$ satisfy (15a). Thus $\mathbf{x}$ must be the unique optimizer of $\mathbf{P}_1$. This proves the theorem. ■

C. Proof of Results on Bounds on Social Utility

1) Proof of Theorem 4.2: From Remark 4.1 it is clear that θ estimated using $\mathbf{x}^0$ in `reduceGraph()` has the property that $\mathbf{x}(t) \leq \theta$ and $\mathbf{z}^*(\mathbf{x}(t)) \leq \theta$, $\forall t \geq 0$ and hence the evolution on $\mathcal{G}$ is same as that on $\hat{\mathcal{F}}$. Suppose $\overline{\mathbf{x}}$ is the steady-state from the initial condition $\mathbf{x}^0$. Then notice that $\overline{\mathbf{x}}$ can be expressed as $\overline{\mathbf{x}}_i = \mathbf{w}_i = \sum_{j \in {}^{\text{in}}\mathcal{R}^i} \mathbf{r}_{ji}$, $\forall i \in \mathcal{V}$ for some $(\mathbf{w}, \mathbf{r})$ which is a feasible solution of $\mathbf{P}_4$. Thus $U(\overline{\mathbf{x}}) \leq U_{\max}$. ■

2) Proof of Lemma 4.11: (By contradiction) Suppose $\exists\, i \in \hat{\mathcal{V}}$, such that $(i,j) \in \hat{\mathcal{A}}$ and $(j,i) \notin \hat{\mathcal{A}}$ but $\overline{\mathbf{x}}_i \neq 0$ for some $\overline{\mathbf{x}} \in \mathcal{L}^+$. Then,

$$u_j(\overline{\mathbf{x}}_j) \overset{\text{a}}{\geq} u_j(\theta_j) \overset{\text{b}}{\geq} u_i(0) \overset{\text{c}}{>} u_i(\overline{\mathbf{x}}_i) \overset{\text{d}}{\geq} u_j(\overline{\mathbf{x}}_j)\,.$$

Here, inequalities a and c comes from the strict decreasing nature of $u_i(.)$ and $u_j(.)$. Inequality c is strict as $\overline{\mathbf{x}}_i \neq 0$. Inequality b comes from the fact that $(j,i) \notin \hat{\mathcal{A}}$. Inequality d comes from the fact that $(i,j) \in \hat{\mathcal{A}}$ and $\overline{\mathbf{x}} \in \mathcal{NE}_\rho^{|\mathcal{V}|}$. This is a contradiction and the claim of the lemma is hence true. ■

3) Proof of Lemma 4.12: Consider an arbitrary but fixed super node $q \in \Lambda$. First we address the trivial cases. If $\mathcal{M}^q = \mathcal{W}^q$, then (12) is satisfied with $\rho_q^{\max} = 0$ by Lemma 4.11. Also as the total population is *one*, then $\rho_q^{\max} = 1$ is always a valid upper bound on the total fraction in q.

Next we address the case when $\mathcal{W}^q \supset \mathcal{M}^q \neq \emptyset$. As $\mathcal{H}^q$ is a DQCH component of $\hat{\mathcal{F}}$, by Lemma 3.5 if $\overline{\mathbf{x}}_i \neq 0$ for some $i \in \mathcal{W}^q \backslash \mathcal{M}^q$ then $u_i(\overline{\mathbf{x}}_i) \geq u_j(0) = \mathbf{a}_j$, $\forall j \in \mathcal{M}^q$ and hence $u_i(\overline{\mathbf{x}}_i) \geq \mathbf{a}_q^{\max}$. Thus, (12) comes from applying this condition to all nodes $i \in \mathcal{W}^q \setminus \mathcal{M}^q$ such that $\overline{\mathbf{x}}_i \neq 0$. ■

4) Proof of Lemma 4.13: By contradiction Suppose $\exists\, \rho_1, \rho_2 \geq 0$ and $\sigma \in (0,1)$ such that

$$f_{\mathcal{V}'}\Big(\sigma\rho_1 + (1-\sigma)\rho_2\Big) < \sigma f_{\mathcal{V}'}(\rho_1) + (1-\sigma) f_{\mathcal{V}'}(\rho_2)\,. \quad (17)$$

We ignore the trivial cases where $\sigma = 0$ or $\sigma = 1$. Let $\mathbf{x}^1$ and $\mathbf{x}^2$ be the optimizers of $\mathbf{P}_1(\mathcal{V}', \rho_1)$ and $\mathbf{P}_1(\mathcal{V}', \rho_2)$ respectively. Thus, $f_{\mathcal{V}'}(\rho_1) = U(\mathbf{x}^1)$ and $f_{\mathcal{V}'}(\rho_2) = U(\mathbf{x}^2)$. Then it is easy to see that $\sigma\mathbf{x}^1 + (1-\sigma)\mathbf{x}^2$ is a feasible solution of $\mathbf{P}_1(\mathcal{V}', \sigma\rho_1 + (1-\sigma)\rho_2)$. Then,

$$U\Big(\sigma\mathbf{x}^1 + (1-\sigma)\mathbf{x}^2\Big) \leq f_{\mathcal{V}'}\Big(\sigma\rho_1 + (1-\sigma)\rho_2\Big)$$
$$< \sigma f_{\mathcal{V}'}(\rho_1) + (1-\sigma) f_{\mathcal{V}'}(\rho_2) = \sigma U(\mathbf{x}^1) + (1-\sigma) U(\mathbf{x}^2).$$

Here the first inequality comes from the fact that $f_{\mathcal{V}'}\Big(\sigma\rho_1 + (1-\sigma)\rho_2\Big)$ is the optimum of $\mathbf{P}_1(\mathcal{V}', \sigma\rho_1 + (1-\sigma)\rho_2)$. The second strict inequality comes from (17). This contradicts the strict concave nature of $U(.)$ and hence completes the proof. ■

5) Proof of Theorem 4.14: Note that the main steps of the process are illustrated in Algorithm 5. By Remark 4.1, we know that $\hat{\mathcal{F}}$ in Step 1 computes an ICRG of $\mathcal{G}$ and that the evolution of the population is unaffected by it. Next Step 2 computes a MAC partition of $\hat{\mathcal{F}}$, the accuracy of which is demonstrated in Remark 4.8. Γ in Step 3 is the corresponding MAC-SG. By Lemma 4.12, $\rho_q^{\max}$ is an upper bound on the population fraction in each super node for every state in the positive limit set (say $\mathcal{L}^+$) of the trajectory starting from $\mathbf{x}^0$. Thus, every $\overline{\mathbf{x}} \in \mathcal{L}^+$ can be written as a feasible solution for $\mathbf{P}_5$. Moreover, inside each super node, the steady-state social utility is given by $\mathbf{P}_1$. Hence the lower bound holds. ■

Nirabhra Mandal received the B.Tech. degree in Electrical Engineering from Institute of Engineering and Management, Salt Lake, Kolkata, India in 2017. Since 2018, he is pursuing the M.Tech(Res) degree from the Department of Electrical Engineering at the Indian Institute of Science. His research interests include multi-agent systems, population games, evolutionary dynamics on networks and non-linear control.

Pavankumar Tallapragada (S'12-M'14) received the B.E. degree in Instrumentation Engineering from SGGS Institute of Engineering & Technology, Nanded, India in 2005, M.Sc. (Engg.) degree in Instrumentation from the Indian Institute of Science in 2007 and the Ph.D. degree in Mechanical Engineering from the University of Maryland, College Park in 2013. He was a Postdoctoral Scholar in the Department of Mechanical and Aerospace Engineering at the University of California, San Diego from 2014 to 2017. He is currently an Assistant Professor in the Department of Electrical Engineering and the Robert Bosch Centre for Cyber Physical Systems at the Indian Institute of Science. His research interests include networked control systems, distributed control, multi-agent systems and networked transportation systems.